REPORT No. 910

SUMMARY OF DRAG CHARACTERISTICS OF PRACTICAL-CONSTRUCTION WING SECTIONS

By John H. Quinn, Jr.

SUMMARY

The effects of several parameters on the drag characteristics of practical-construction wing sections have been considered and evaluated. The effects considered were those of surface roughness, surface waviness, compressive load, and de-icers. The data were obtained from a number of tests in the Langley two-dimensional low-turbulence tunnels.

The section drag coefficients of practical-construction wings in the "as-received" condition were often as high as 0.0070 at Reynolds numbers of 20×10^6. When spar joints or surface unfairness occurred in a region of normally laminar flow, decreases in section drag coefficient up to 50 percent could be obtained by a combination of surface finishing and fairing. In some cases, nearly half this improvement was due to better surface fairness. The drag of smooth wings with thick skin having spars placed at or behind the most rearward position at which laminar flow might be expected approached that of fair and smooth airfoils of corresponding sections. Some quantitative data were obtained and indicated the effects of waves in the laminar-flow region of smooth practical-construction wings on the Reynolds number at which premature transition would occur. For Reynolds numbers up to 50×10^6, a few examples are given of surface waves on NACA 6-series airfoil sections that did not cause premature transition.

As a result of the construction irregularities existing on wings as received from the manufacturer, the differences in drag usually associated with airfoils of different series were not obtained. Combinations of glazing, painting, or minor refairing of the surfaces, however, were sufficient to produce section drag coefficients approaching those for fair and smooth airfoils of corresponding sections at Reynolds numbers up to approximately 20×10^6.

Loading a wing in compression until some slight permanent set of the skin or rivets occurred had little or no adverse effect on the drag characteristics of two wing sections designed to retain their true contours under loads usually encountered in flight. While the wing was under load sufficient to produce such deformation, however, drag coefficients as high as 0.0060 were obtained at a Reynolds number of approximately 24×10^6 as compared with a value of 0.0045 for the unloaded wing at the same Reynolds number.

Airfoil sections having thickness ratios of approximately 15 percent and equipped with leading-edge de-icer boots were found to have section drag coefficients of approximately 0.0070 at Reynolds numbers between 10×10^6 and 32×10^6. This value of the section drag coefficient appeared to be independent of the airfoil section upon which the de-icer was mounted.

INTRODUCTION

Numerous investigations of airfoil sections built by various practical-construction methods have been made in the Langley two-dimensional low-turbulence tunnels to determine the effects of construction irregularities on the aerodynamic characteristics of the airfoil sections that each model represented. The results of the tests were useful in estimating performance characteristics of the airplane for which each installation was being considered, but no attempt was made to correlate the aerodynamic characteristics of the wing sections with the type of construction employed.

In the present paper the data obtained from the tests have been collected and analyzed to find the effects of several parameters on the drag characteristics of practical-construction wings. The effects of surface roughness, surface waviness, compressive load, and de-icers were considered. The drag characteristics of the models, which represented both NACA 6- and 230-series airfoil sections, were obtained for various surface conditions. These surface conditions generally included the original condition as received from the manufacturer and a number of improved conditions obtained by glazing, sanding, painting, or by a combination of these processes. Surface-waviness measurements were made more recently on several models and the drag and waviness measurements were correlated wherever possible.

SYMBOLS

c	airfoil chord, feet
d	difference between gage reading on airfoil surface and on a flat plate, feet
d/c	waviness index
s	chordwise distance along airfoil surface from leading edge, feet
c_d	section drag coefficient
c_l	section lift coefficient
c_{l_i}	design section lift coefficient
R	Reynolds number based on wing chord
g	acceleration of gravity, feet per second per second
x	distance along chord from leading edge, feet
δ	effective thickness of boundary layer; thickness to point where velocity inside boundary layer is equal to 0.707 of velocity outside boundary layer, feet
R_δ	Reynolds number based on effective boundary-layer thickness

U	local velocity outside boundary layer, feet per second
U_0	free-stream velocity, feet per second
S	pressure coefficient $\left(\frac{H_0-p}{q_0}\right)$
H_0	free-stream total pressure
p	local static pressure
q_0	free-stream dynamic pressure

MODELS

The models tested were built by practical-construction methods and were of 3-foot span and from 6- to 8.33-foot chord. Chordwise stiffeners, spanwise stiffeners, or combinations of the two were used, and the models were of the single-, double-, or triple-spar type. Both NACA 230- and 6-series airfoil sections were represented. Explanations of the airfoil designations are included in reference 1.

The original condition of the wing as received from the manufacturer and also the various improved conditions are described for each model where data for the various surface finishes are presented. These improved surface conditions were obtained by one or more of the following finishing procedures:

Camouflage painted: Painted with synthetic-enamel camouflage paint giving a surface condition similar to that obtained by procedure 5 of reference 2.

Sanded: Surface sanded sufficiently to remove paint specks and other similar excrescences.

Glazed: Local defects such as nicks, dimples around rivets, and seams, filled with pyroxylin putty and sanded smooth.

Painted: Painted with gray primer surfacer and sanded smooth with No. 320 carborundum paper.

Faired: Modifications to surface either by extensive application of pyroxylin putty or rebuilding to reduce the number and size of larger surface irregularities.

In the present paper the term "roughness" is used to denote the presence of local nicks or scratches, open seams due to chordwise or spanwise joints, dimples around rivets or screws, paint specks, or other similar projections. The term "waviness" is limited to those wrinkles in the skin that present gentle deviations from a fair surface. A surface is considered to be aerodynamically fair and smooth when further decreases in the amount of surface roughness and waviness produce no change in the aerodynamic characteristics.

Descriptions of the models, a list of the surface conditions studied, and an index to figures in which data for the various surface conditions are contained are presented in table I for the models considered herein.

TEST METHODS

The tests of the practical-construction wing models were made in the Langley two-dimensional low-turbulence tunnel and in the Langley two-dimensional low-turbulence pressure tunnel. These tunnels have test sections 3 feet wide by 7½ feet high and were designed to test models completely spanning the jet in two-dimensional flow. The turbulence level of these tunnels amounts to only a few hundredths of 1 percent and is considerably below that at which any effect is apparent on the critical Reynolds number of a sphere. Tests in the pressure tunnel may be made under pressures ranging from 14.7 to 150 pounds per square inch absolute; therefore, by increasing the tunnel pressure high Reynolds numbers may be obtained at relatively low Mach numbers. The Mach number of the tests was in no case greater than 0.2. In these tunnels, lift is measured by integrating the pressures along the floor and ceiling of the tunnel test section and drag is measured by the wake-survey method. The drag coefficients are usually obtained at a spanwise position selected as a representative section of the wing from a number of spanwise surveys at a low lift coefficient. More detailed descriptions of the methods used in obtaining and reducing data in these tunnels are contained in reference 1.

Surface-waviness measurements for the wind-tunnel models were obtained with a standard Ames dial gage mounted on legs spaced $2\frac{15}{32}$ inches. The readings were reduced to dimensionless form by subtracting the reading of the gage when placed on a flat surface from the readings obtained with the gage in various positions along the airfoil surface and dividing the difference by the airfoil chord.

RESULTS AND DISCUSSION

In the analysis of the effects of surface roughness and waviness, the surfaces were assumed to be so smooth that the differences observed between the measured drags and the drags of fair and smooth models were related directly to the relative extents of the laminar and turbulent boundary layers. The effects of surface roughness or waviness on drag therefore can be interpreted essentially as the effect of this roughness or waviness on the position of the transition from the laminar to the turbulent layer.

In order to derive an approximate relation between the section drag coefficient and the position of transition, section drag coefficients have been calculated by the method of reference 3 for the NACA $66_{(215)}$-116 airfoil section at a section lift coefficient of 0.1 and a Reynolds number of 20×10^6 for assumed positions of transition ranging from $0.1c$ to $0.6c$. (See fig. 1.) These calculated values have been used throughout the analysis when an estimate of the transition point on NACA 6-series airfoils was required, since the variation shown in figure 1 is thought to be reasonably representative of the airfoil sections for which data are presented herein. The values of the section drag coefficient found for transition at $0.50c$ or $0.60c$ are probably slightly higher than those of fair and smooth NACA 65- or 66-series airfoils, respectively, because at Reynolds numbers up to approximately 20×10^6 transition would probably occur slightly behind the minimum pressure point.

EFFECTS OF SURFACE CONDITIONS

Surface roughness.—In the consideration of the effects of surface roughness on the drag characteristics of practical-construction wings, the separate effects of various steps in the finishing process have been determined. Photographs of models 1 to 6, which are NACA 6-series airfoil sections, are presented as figures 2 to 7. The drag characteristics of these models with various surface conditions are presented in figure 8.

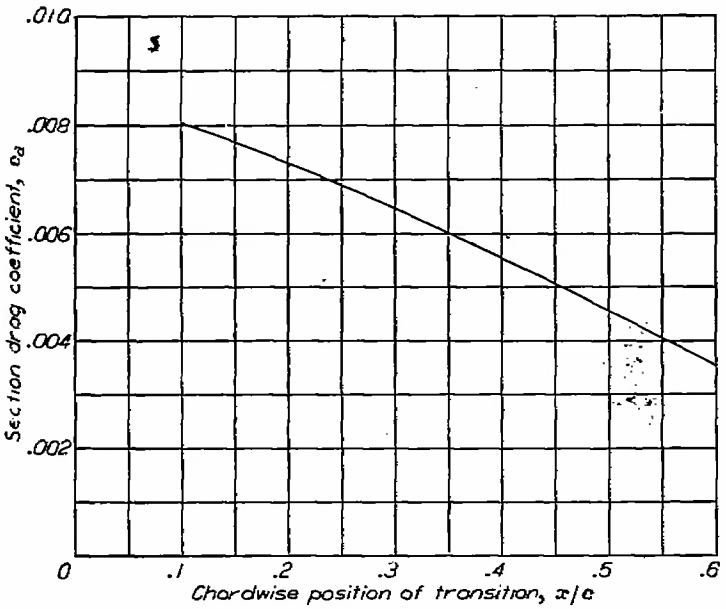

FIGURE 1.—Calculated variation of section drag coefficient with position of transition on NACA 66(na)-116 airfoil section. $c_l=0.1$; $R=20\times10^6$.

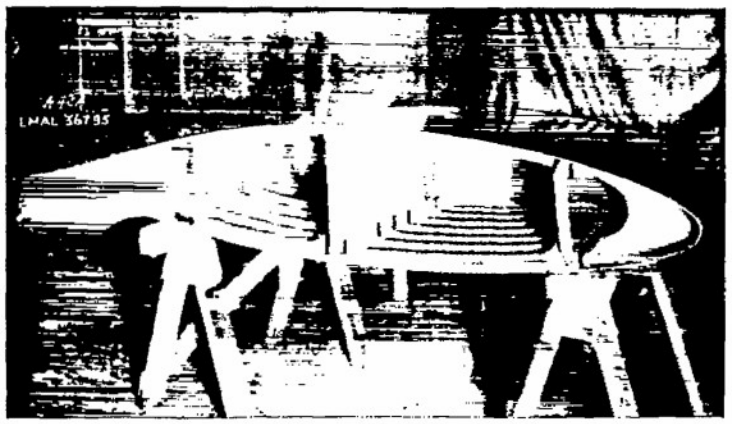

FIGURE 2.—Model of NACA 65(216)-3(16.5) (approx.) practical-construction airfoil section with bare-metal surfaces. Model 1.

From figure 8 (a) at a Reynolds number of 20×10^6 the following drag characteristics may be obtained for model 1 (NACA 65(216)-3(16.5) (approx.) airfoil section):

Step	Surface condition	c_d	Percentage improvement
1	Original camouflage painted; discontinuity at front spar (0.12c)	0.0086	
2	Upper surface glazed over front spar; lower surface glazed to front spar	.0070	19
3	Upper surface painted to 0.71c; lower surface painted to 0.12c	.0058	32
4	Both surfaces painted to 0.71c	.0052	40

An irregularity consisting of a rather large flat spot existed at the front spar (0.12c) on both surfaces in the original condition. This flat spot was detected by rocking a straightedge over the surfaces in a chordwise direction. The large reduction in drag obtained from step 2 was probably due to a partial fairing of the flat spot on the upper surface. Transition moved downstream but still occurred forward of the minimum pressure point as a result of the flat spot. Local glazing (step 2) and painting the model surfaces (steps 3 and 4) are not thought to alter the surface waviness appreciably but rather to eliminate local nicks, dimples, seams, and scratches. The final value of the section drag coefficient of 0.0052 obtained with step 4 corresponds to transition at approximately 0.43c, or 0.07c ahead of the design position of minimum pressure on an NACA 65-series airfoil section. Since the model surfaces after step 4 were smooth and the middle spar was located at 0.45c, the remaining unfairness near the nose of the model appeared to be responsible for the premature transition.

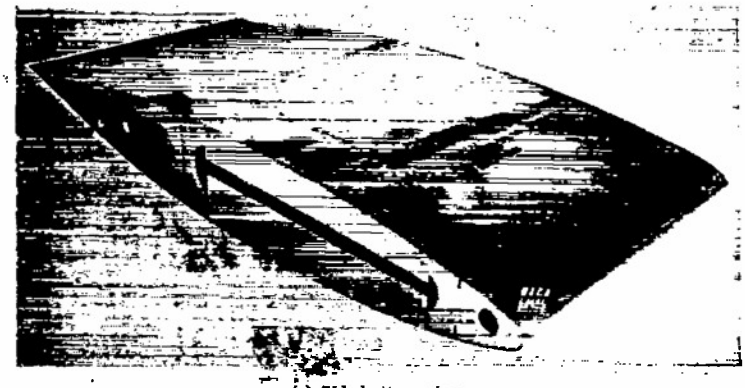

(a) Side bottom view

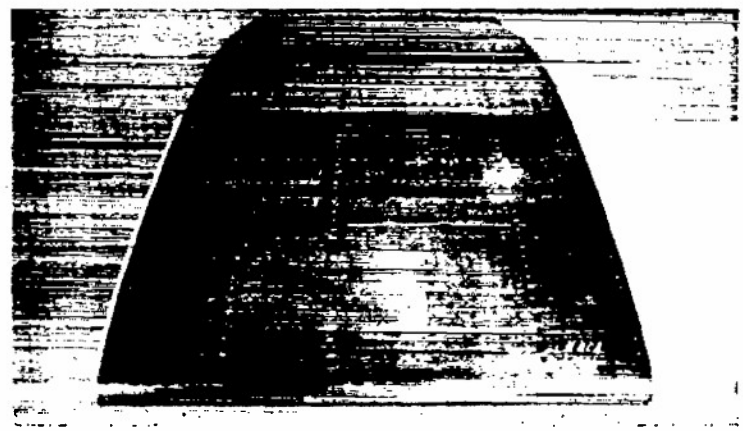

(b) Front top view.

FIGURE 3.—Model of NACA 66(215)-214 (approx.) practical-construction airfoil section with unpainted surfaces. Model 2.

FIGURE 4.—Model of NACA 66(215)-116 practical-construction airfoil section with local surface defects glazed. Model 3.

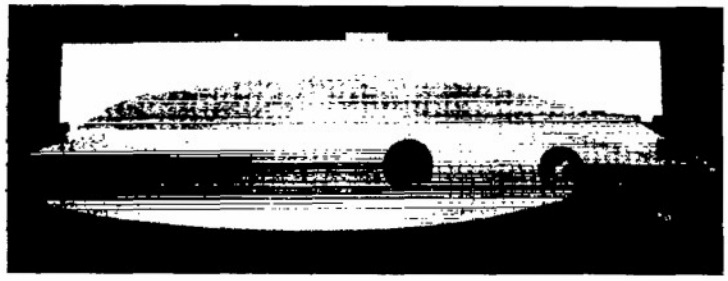

(a) Upper-surface templet.

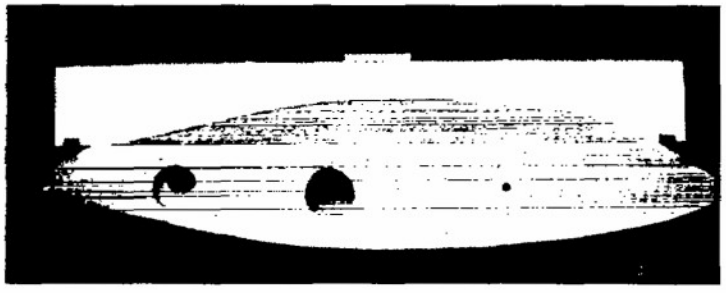

(b) Lower-surface templet.

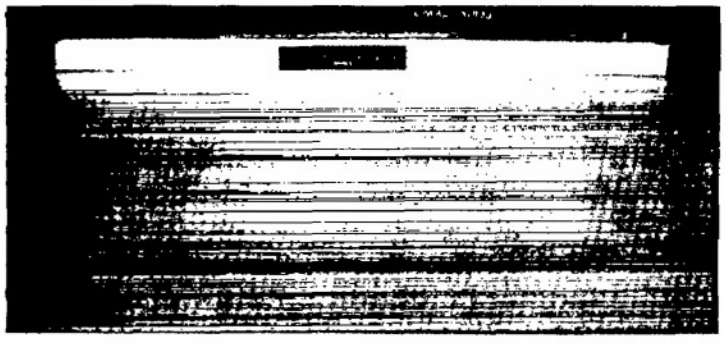

(c) Spanwise variation in contour.

FIGURE 5.—Model of NACA 66(215)-116 $\left\{\begin{matrix} a=1.0,\ c_{l_i}=0.2 \\ a=0.6,\ c_{l_i}=-0.1 \end{matrix}\right\}$ practical-construction airfoil section. Model 4.

The following table shows the improvements made on model 2 (NACA 66(215)-214 (approx.) airfoil section) at a Reynolds number of 20×10^6, as obtained from figure 8 (b):

Step	Surface condition	c_d	Percentage improvement
1	Original, unpainted	0.0070	--------
2	Glazed and painted	.0055	21
3	Refaired	.0035	50

The drag was reduced 50 percent, although a reduction of only 21 percent was obtained by smoothing the surfaces. In the unpainted condition, the section drag coefficient of 0.0070 corresponds to transition at approximately 0.24c. Figure 3 shows that numerous dimples caused by the rivets existed in the skin. These dimples were probably responsible for transition approximately 0.10c ahead of the front spar. Glazing and painting the model reduced the section drag coefficient to 0.0055 or moved transition to approximately 0.40c. Transition at this point was probably due to unfairness at the front spar. Refairing the model evidently removed

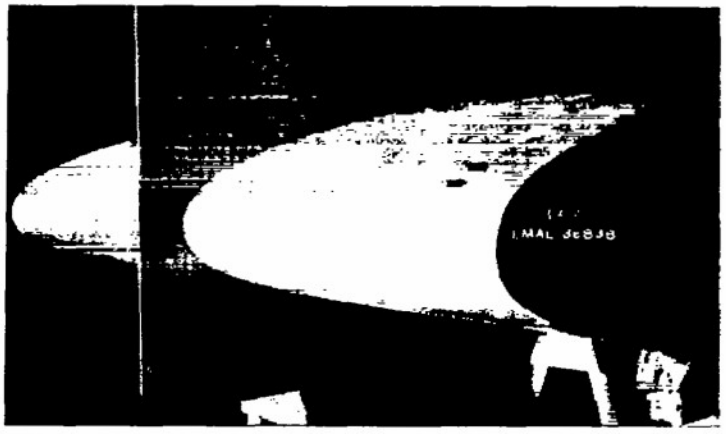

(a) Nose templet, model erect.

(b) Nose templet, model inverted.

FIGURE 6.—Model of NACA 66(215)-116 $\left\{\begin{matrix} a=1.0,\ c_{l_i}=0.2 \\ a=0.6,\ c_{l_i}=-0.1 \end{matrix}\right\}$ practical-construction airfoil section with surfaces painted with zinc-chromate primer. Model 5.

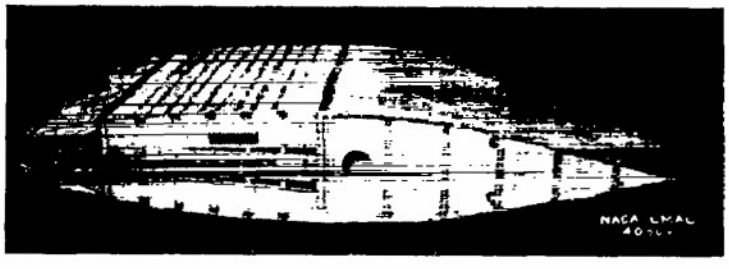

FIGURE 7.—Model of NACA 66(215)-116 practical-construction airfoil section with surfaces glazed and smooth to rear spar. Model 6.

the irregularity at the front spar and the section drag coefficient was reduced to the value of 0.0035, or approximately the same as that of a fair and smooth model of the same section.

The drag characteristics of model 3 (NACA 66(215)-116 airfoil section) are presented in figure 8 (c) for a range of Reynolds numbers and in the following table for a Reynolds number of 20×10^6:

Step	Surface condition	c_d	Percentage improvement
1	Original (bare metal skin)	0.0062	--------
2	Glazed to spar joint at 0.32c	.0055	11
3	Glazed and painted over spar joint	.0044	29
4	Entire surface painted	.0042	32
5	Partly refaired	.0040	36

The section drag coefficient of the model in the original (bare metal) condition, 0.0062, corresponds to transition at approximately 0.32c. Dimples and local defects forward of the spar (fig. 4) probably caused transition at that point. The glazing of the surfaces forward of the spar (step 2) reduced the drag 11 percent; the section drag coefficient of 0.0055 corresponds to transition at about 0.40c. Glazing and painting over the spar joint (step 3) decreased the section drag coefficient to 0.0044 or moved transition to approximately 0.50c. Painting the entire model surfaces (step 4) brought about little further improvement. Some waviness at the spar joint at 0.32c (table I) was probably responsible for premature transition on model 3. The final section drag coefficient of 0.0040, however, shows that the waviness did not cause premature transition up to approximately 0.55c.

The drag characteristics of model 4 $\left(\text{NACA } 66(215)\text{-}116 \begin{Bmatrix} a=1.0, c_{l_i}=0.2 \\ a=0.6, c_{l_i}=-0.1 \end{Bmatrix} \text{airfoil section}\right)$ are presented in figure 8(d) and in the following table at a Reynolds number of 20×10^6:

Step	Surface condition	c_d	Percentage improvement
1	Original—painted with zinc-chromate primer	0.0056	
2	Painted	.0040	29
3	Glazed	.0040	29

A total reduction in section drag coefficient from 0.0056 to 0.0040, or 29 percent, was obtained by smoothing the model surfaces. The sudden increase in section drag coefficient at a Reynolds number of 13×10^6 was thus eliminated, as shown in figure 8 (d). Rapid increases in section drag coefficient with Reynolds number, similar to that shown, are usually associated with surface roughness. Local nicks or depressions near the rivets probably caused premature transition at a Reynolds number of 13×10^6 in the unpainted condition but were not large enough to cause premature transition at lower Reynolds numbers. The flush riveting on this model was unusually smooth. The final section drag coefficient of 0.0040 is higher than that of a fair and smooth NACA 66-series airfoil section. Because the spar on this model was located at 0.60c (table I), waviness at the spar joint was not likely to be responsible for this discrepancy. Deviations from true contour in both the chordwise and spanwise directions, as shown in figure 5, therefore, were probably responsible for the slightly higher drags in the finished condition.

The section drag coefficient of 0.0037 for model 5 $\left(\text{NACA } 66(215)\text{-}116 \begin{Bmatrix} a=1.0, c_{l_i}=0.2 \\ a=0.6, c_{l_i}=-0.1 \end{Bmatrix} \text{airfoil section}\right)$ found at $R=20\times10^6$ (fig. 8 (e)) is nearly the same as that of a fair and smooth 66-series section, and consequently little or no improvement was made by painting and sanding. The spar location at 0.60c combined with the use of a thick skin (table I), probably made possible the realization of low-drag characteristics to higher Reynolds numbers than have been found with most models having spars located farther forward.

Variations of section drag coefficient with surface condition for model 6 (NACA 66(215)-116 airfoil section) are shown in the following table at a Reynolds number of 20×10^6, as obtained from figure 8 (f):

Step	Surface condition	c_d	Percentage improvement
1	Original—covered with fabric surfacer	0.0066	
2	Fabric surfacer sanded	.0060	9
3	Surfacer removed	.0072	−9
4	Glazed up to 0.15c	.0072	−9
5	Glazed up to 0.45c	.0066	0

No large decreases in section drag coefficient were obtained by improving the surface finish of model 6. In the best condition—that is, with fabric surfacer sanded—transition probably occurred at approximately 0.35c, or 0.25c ahead of the design position of minimum pressure. The surface material, which consisted of fabric doped to the metal skin, evidently masked considerable unfairness, for in the bare-metal condition the drag was 9 percent higher than that for the model in the original condition. The drag coefficient of 0.0072 for steps 3 and 4 would correspond to transition at approximately 0.21c. Glazing to the rear spar (step 5) resulted in a section drag coefficient that would correspond to transition at about 0.28c. The model surfaces in this case were very smooth; the extreme surface waviness of model 6, therefore, was probably responsible for the high section drag coefficients.

The preceding observations of the decrease in drag caused by improving the surface finish and fairness of practical-construction wings at a Reynolds number of 20×10^6 are summarized in the following statements: When spar joints or similar surface irregularities occurred in a region of normally laminar flow, the section drag coefficients of several NACA 6-series airfoil sections as received from the manufacturer ranged from 0.0062 to 0.0086. A combination of improvement in surface smoothness and fairness obtained by glazing, painting, or minor refairing reduced these section drag coefficients by an amount ranging from 0.0022 to 0.0035, depending upon the value of the original drags. Tests of two models having thick skins and spars placed at or behind the most rearward position at which laminar flow might be expected yielded section drag coefficients very close to those of fair and smooth airfoils of corresponding sections. Elimination of minor surface roughness by local glazing and painting helped to maintain these values of the section drag coefficient over a rather large range of Reynolds number. Glazing and painting these models did not, however, eliminate the adverse effects of surface unfairness or waviness where it existed, although the severity of these effects was usually lessened.

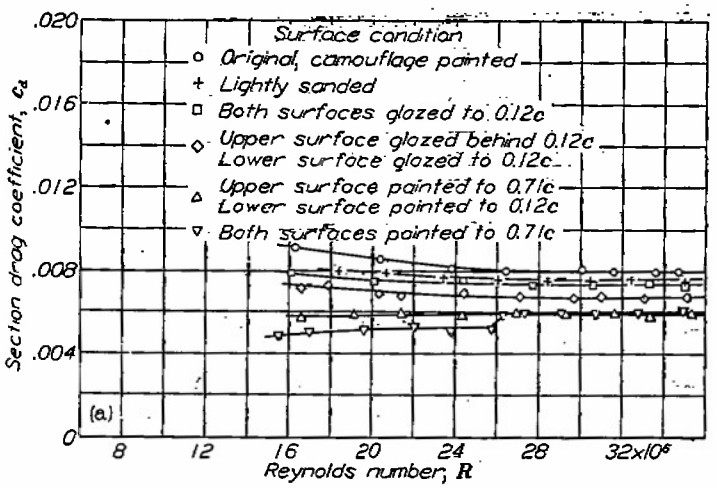

(a) Model 1, NACA 65(216)-3(16.5) (approx.) airfoil section. c_l=0.2.

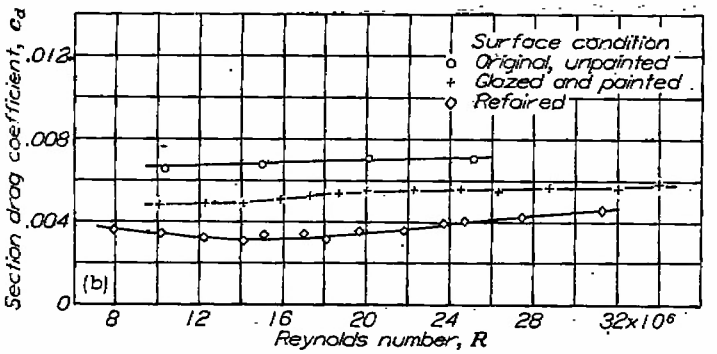

(b) Model 2, NACA 66(215)-214 (approx.) airfoil section. c_l=0.18.

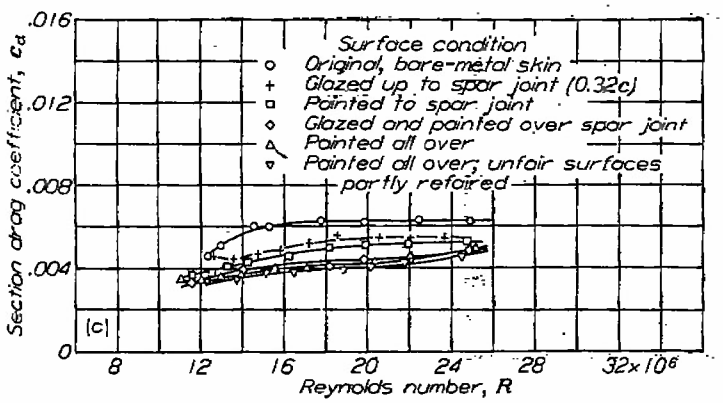

(c) Model 3, NACA 66(215)-116 airfoil section. c_l=0.18.

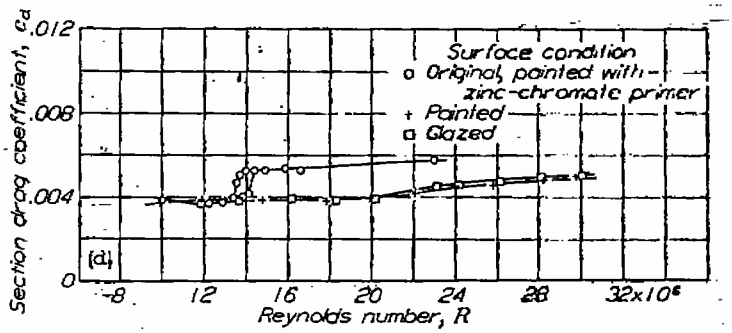

(d) Model 4, NACA 66(215)-116 $\begin{cases}\alpha=1.0,\ c_{l_i}=0.2\\ \alpha=0.6,\ c_{l_i}=-0.1\end{cases}$ airfoil section. c_l=0.1.

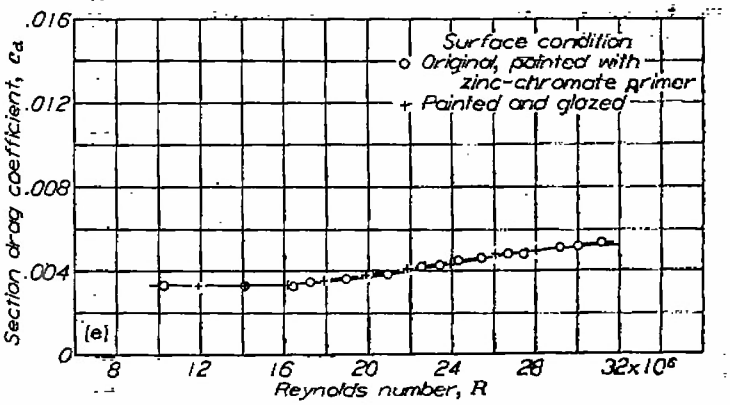

(e) Model 5, NACA 66(215)-116 $\begin{cases}\alpha=1.0,\ c_{l_i}=0.2\\ \alpha=0.6,\ c_{l_i}=-0.1\end{cases}$ airfoil section. c_l=0.1.

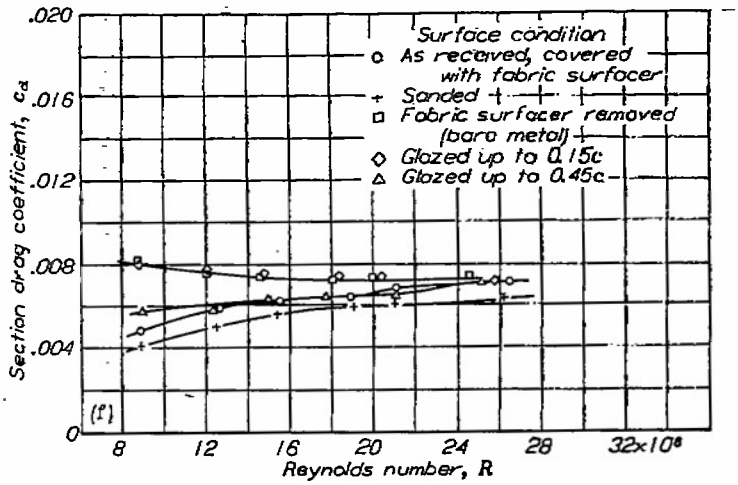

(f) Model 6, NACA 66(215)-116 practical-construction airfoil section. c_l=0.15 (approx.).

FIGURE 8.—Effect of surface improvements on drag characteristics of airfoil sections.

Surface waviness.—In the consideration of the effects of surface waviness on the drag characteristics of airfoil sections, the effects of roughness have been eliminated by using data for smooth models only. The types of waviness investigated were those associated with short-wave-length wrinkles in the airfoil skin and with deviations from true contour over a large part of the chord. The wrinkles, or waves, were detected by passing a surface gage over the airfoil surface to obtain the waviness index d/c at a number of chordwise locations. Any deviation from a fair curve in the plot of waviness index against chordwise position is an indication of a surface wave, although the waviness index does not give directly either the length or magnitude of the wave. When the spacing of the legs of the gage is approximately a constant fraction of the airfoil chord, however, the deviation of the chordwise variation of the waviness index from a fair curve is a satisfactory means of comparing the relative waviness on different airfoil models. Deviations from true airfoil contour over a large part of the airfoil chord were investigated in one case by checking the model contour with a templet. Feeler gages inserted between the templet and the airfoil surface were used to measure the deviation from the true contour.

The surface waviness on two models was reduced beyond the point where an effect on drag was noticeable. The two models were model 7 (the NACA $66_{(215)}$–114 airfoil section) and model 8 (the NACA 66(2x15)–116 airfoil section). The drag characteristics of models 7 and 8 could then be compared with those of other smooth models of similar airfoil section to determine whether the drag characteristics of the other models were adversely affected by surface waviness and, if so, to what extent.

A photograph of model 7 is presented as figure 9. The drag characteristics of this model with two conditions of surface waviness are presented in figure 10, and the waviness measurements for the two surface conditions are presented in figure 11. Almost no difference was found in the drag characteristics with the two waviness conditions, although inspection of figure 11 shows that in the faired condition the model surfaces were considerably more fair than in the "as-received" condition. Because a marked reduction in the surface waviness thus had no apparent effect on the drag characteristics of model 7, it was thought that transition probably moves forward as the Reynolds number increases even if no waves exist. In order to investigate the possibility of this phenomenon, drag coefficients were calculated for several Reynolds numbers by the method of reference 3. For these calculations it was assumed that transition would occur at a constant value of R_δ (Reynolds number based on the effective boundary-layer thickness) unless the particular value of R_δ chosen occurred behind the position of minimum pressure. Estimation of the transition point in an adverse pressure gradient is rather involved and was not considered of sufficient interest in the present paper to be included.

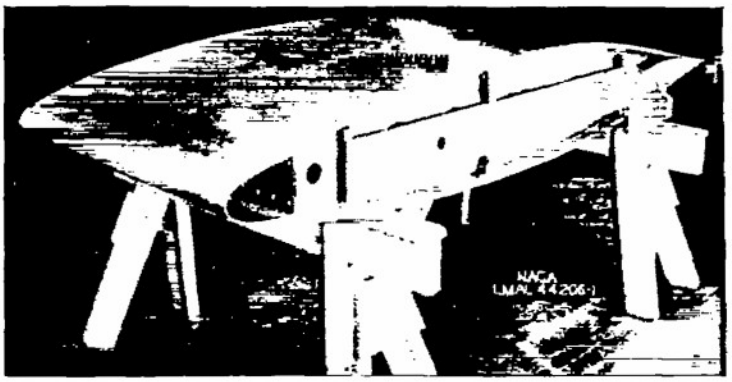

FIGURE 9.—Three-quarter front view of upper surface of NACA $66_{(215)}$-114 airfoil section in as-received condition. Model 7

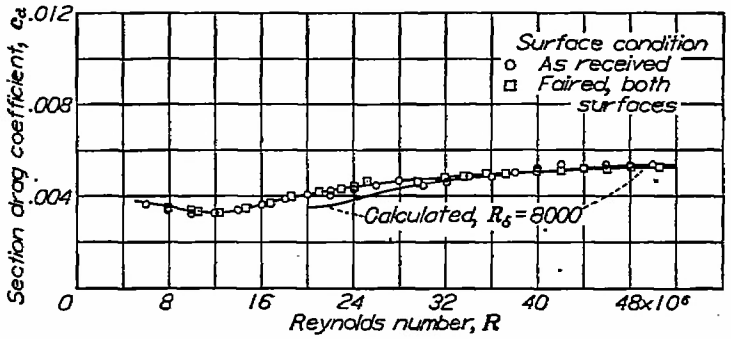

FIGURE 10.—Experimental and calculated section drag characteristics for NACA $66_{(215)}$-114 practical-construction airfoil section. c_l=0.1 (approx.). Model 7.

The position of transition was estimated for several assumed values of R_δ between 6500 and 8500 by use of the following equation obtained from reference 4:

$$\frac{R_\delta^2}{R}=(2.3)^2\left(\frac{U_0}{U}\right)_x^{7.17}\int_0^x\left(\frac{U}{U_0}\right)^{8.17}d\frac{s}{c}$$

The use of a constant value of R_δ of 8000 was found to provide the best over-all agreement between the calculated and experimental section drag coefficients. Although the calculated-drag and experimental-drag curves of figure 10 do not agree very closely at Reynolds numbers between 20×10^6 and 30×10^6, the section drag coefficients obtained experimentally and theoretically are in good agreement for Reynolds numbers between 30×10^6 and 50×10^6. At Reynolds numbers between 20×10^6 and 30×10^6, the higher drags of the experimental results could have been caused by very small particles of lint and dust adhering to the airfoil surface. The model surfaces were partly painted and glazed and partly bare metal for the faired condition. In the past, unpolished metal surfaces have often been found to present greater difficulties in eliminating dust and other particles than do high-gloss or polished surfaces. An accumulation of small dust particles could bring about small disturbances in the laminar-flow layer that would produce slight premature forward movements of transition.

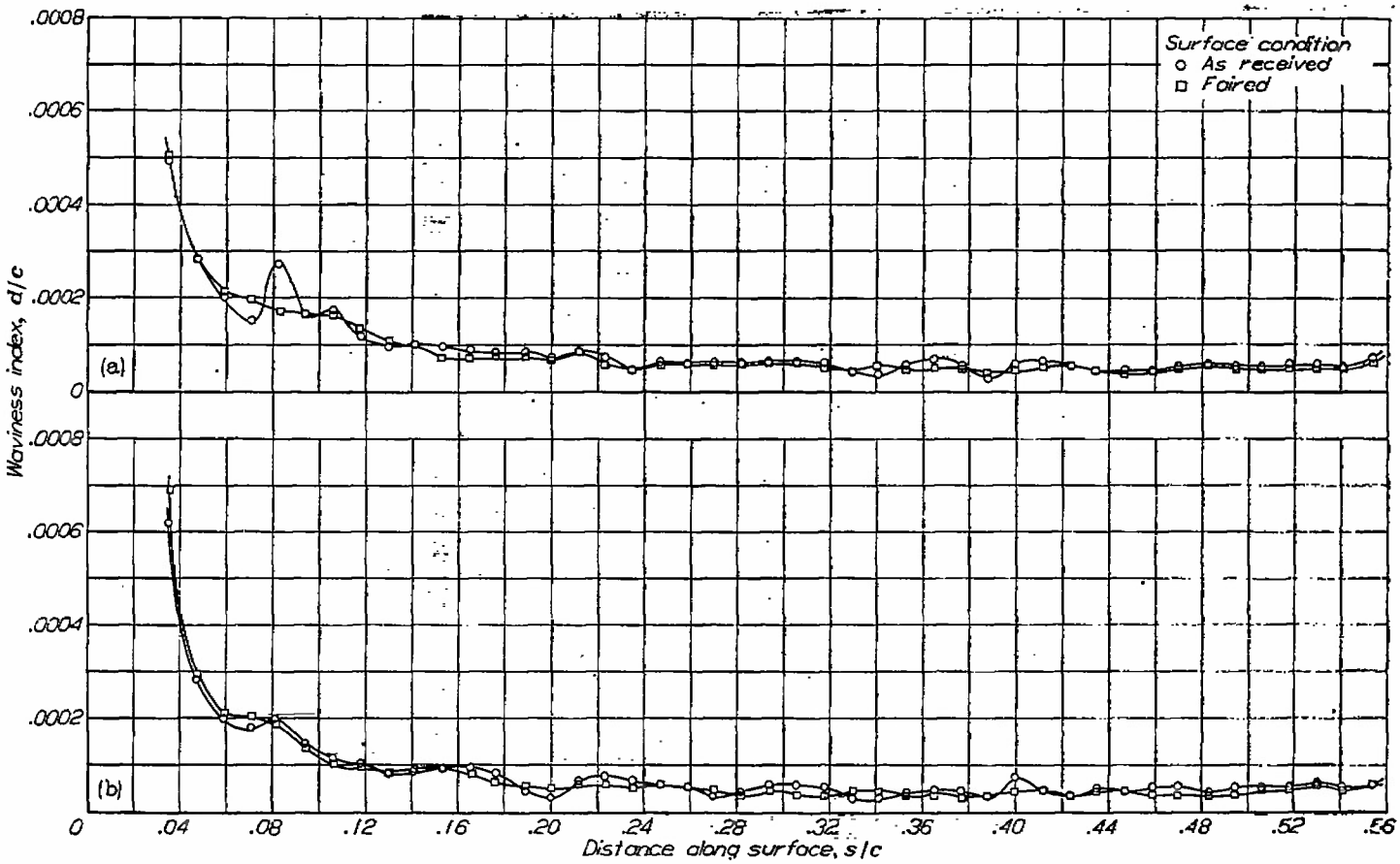

(a) Upper surface.
(b) Lower surface.

FIGURE 11.—Waviness characteristics of NACA 66(2x15)-114 practical-construction airfoil section in as-received condition and in faired condition. Model 7.

Although the value of R_δ of 8000 was obtained by trial and error in an attempt to obtain correlation between the experimental and calculated curves, reference 4 indicated that under one set of conditions transition was found to occur on an airplane wing in flight at values of R_δ between 8000 and 9500.

Drag-scale-effect curves were also obtained for model 8 (the NACA 66(2x15)-116 airfoil section) under two conditions of surface waviness. A photograph of this model is presented as figure 12, drag characteristics are presented in figure 13, and waviness measurements are presented in figure 14. With the airfoil camouflage painted and sanded, considerable waviness existed near the front spar located at 0.35c (fig. 14). A reduction in waviness at that point had a very small effect on the drag characteristics, bringing about a reduction in section drag coefficient of approximately 0.0002 at Reynolds numbers between 30×10^6 and 50×10^6 (fig. 13). In the faired condition, the model surfaces were approximately as fair as it was practically feasible to make them. Calculated drag curves for critical values of R_δ of 8000, 8500, and 9000 are presented, together with experimental data, in figure 13. Very good agreement was obtained between the experimental values and the calculated values for R_δ=9000.

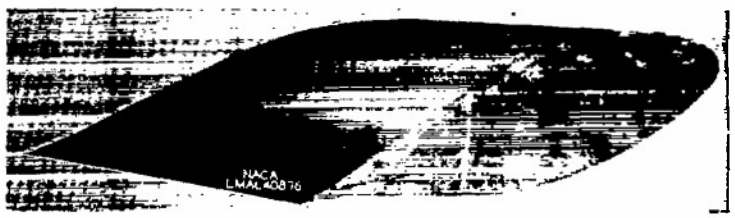

FIGURE 12.—Model of NACA 66(2x15)-116 practical-construction airfoil section with camouflage-painted surfaces. Model 8.

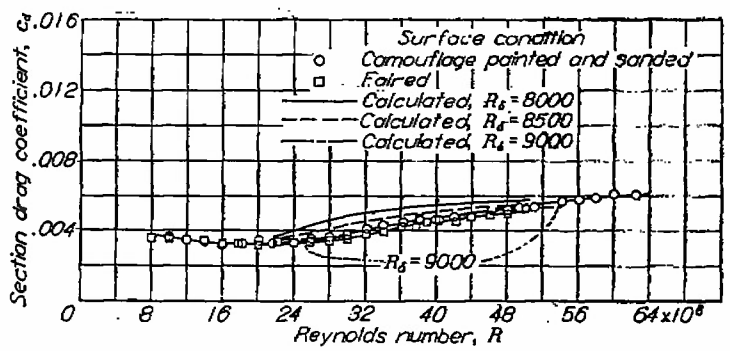

FIGURE 13.—Comparison of experimental and calculated drag-scale-effect curves for NACA 66(2x15)-116 practical-construction airfoil section. c_l=0.1. Model 8.

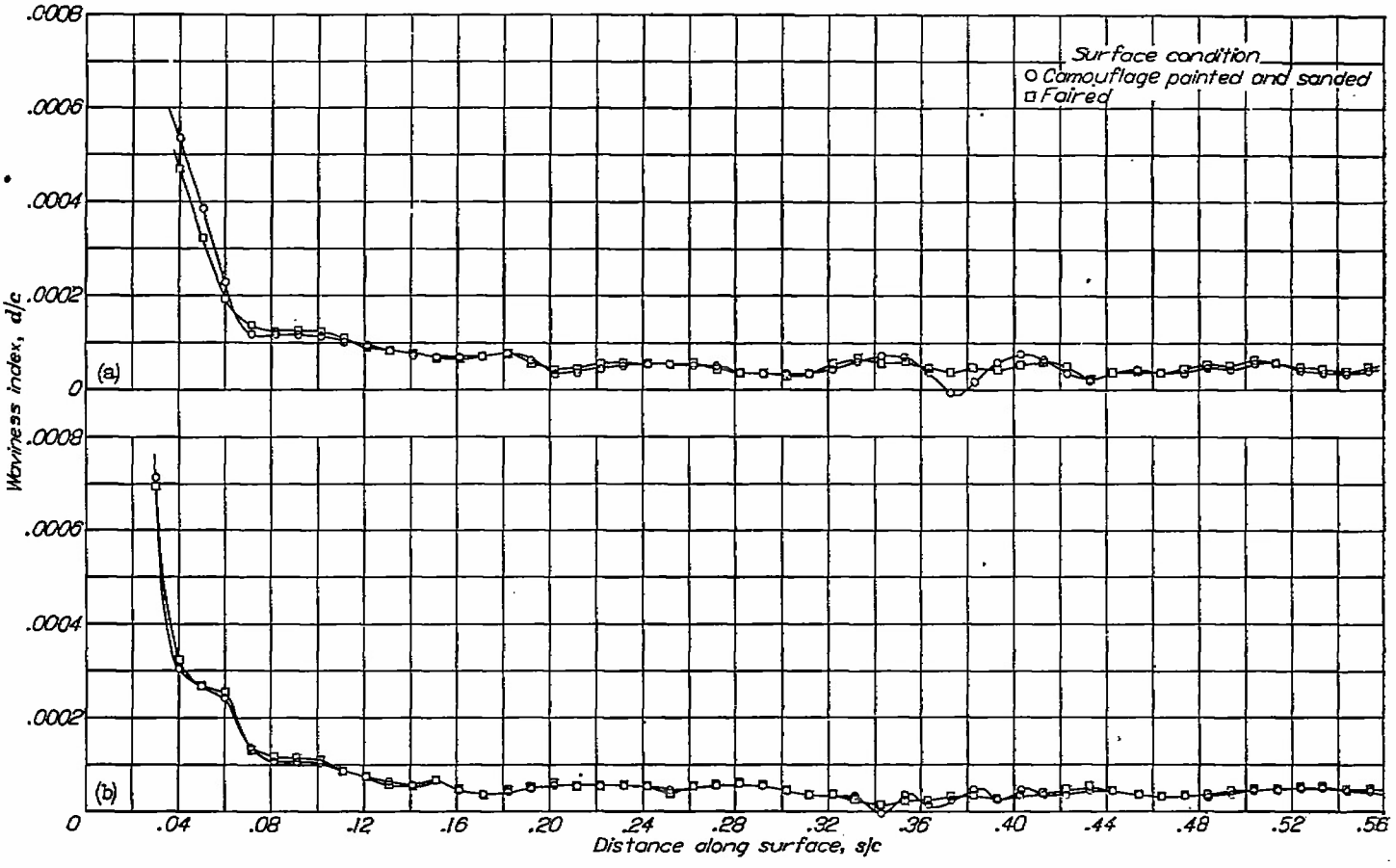

(a) Upper surface.
(b) Lower surface.

FIGURE 14.—Waviness characteristics of NACA 66(2x15)-116 practical-construction airfoil section before and after fairing process. Model 8.

Because it was possible to calculate for model 8 both the value of the Reynolds number at which minimum drag occurred and the value of the section drag coefficients at high Reynolds numbers, it appears that it is possible to approximate the drag-scale-effect curve for a smooth and fair airfoil by assuming that transition occurs at a critical value of R_s between 8000 and 9000 when it does not occur as a result of reversal in the pressure gradient. Because reductions in the amount of surface waviness brought about little measurable change in section drag coefficient, the waviness existing on either model 7 or model 8 did not appear to be sufficiently great to effect the drag characteristics of these airfoils at least at Reynolds numbers between 30×10^6 and 50×10^6.

The drag characteristics of a number of smooth NACA 6-series practical-construction airfoil sections were compared with those of models 7 and 8. Any models for which the drag coefficients fell in the range between the drag coefficients for models 7 and 8, which have been shown to be free of harmful waviness, could also be considered reasonably free of harmful waviness. Any model for which the drag coefficients were greater than those of model 7, on the other hand, were thought to have sufficient waviness to induce premature transition.

A photograph of model 11, the NACA 66,2–115 airfoil section, is presented as figure 15, and the drag characteristics of models 5, 6, 7, 8, 9 (the NACA 66(215)–(1.25)16), 10 (the NACA 66,2–115), and 11 (the NACA 66,2–115) are presented in figure 16. The waviness measurements for models 5, 6, 9, 10, and 11 are presented in figure 17.

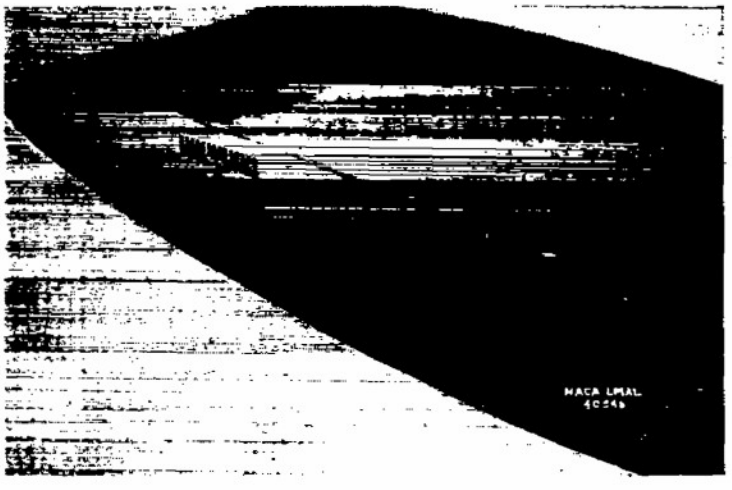

FIGURE 15.—Model of NACA 66, 2-115 practical-construction airfoil section with camouflage-painted surfaces. Model 11. (Model 10 has similar internal structure.)

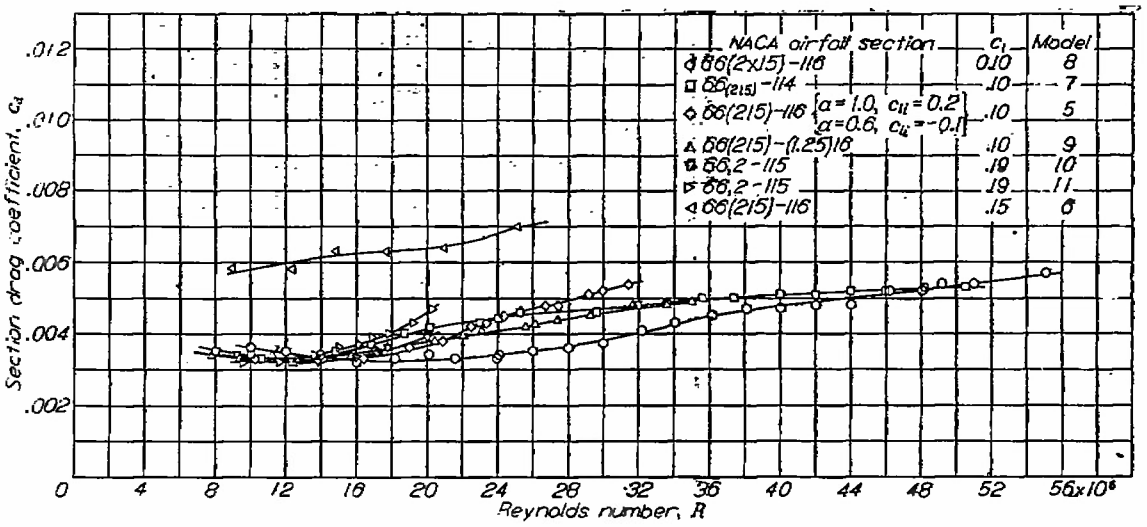

FIGURE 16.—Drag characteristics of some smooth NACA 6-series practical-construction airfoil sections.

With the exception of model 6 all the airfoils for which data are presented in figure 16 had the same value of minimum section drag coefficient. The drag-scale-effect curve for model 5 rose above that for model 7 at a Reynolds number of 24×10^6. Figure 17 (a) shows that model 5 had rather large waves near the leading edge on both surfaces. Waves near the leading edge that produce variations in the waviness index similar to the variations shown in figure 17 (a) can be considered representative of those that would have an adverse effect on the position of transition, at least for Reynolds numbers between 24×10^6 and 32×10^6. The drag-scale-effect curves for models 9 and 10 fell between those for models 7 and 8. The waves existing on models 9 and 10 were probably not sufficiently large to cause premature transition over the Reynolds number range for which data were obtained. The waviness data for models 9 and 10 presented in figures 17 (b) and 17 (c), respectively, give examples of permissible waviness if premature transition is to be avoided up to Reynolds numbers of at least 35×10^6 and 20×10^6, respectively. The section drag coefficients of model 11 (fig. 16) were greater than those of model 7 at Reynolds numbers above 16×10^6. Figure 17 (d) shows that waves existing on model 11 produced a number of large variations in the waviness index. Such waviness may be considered as representative of that which will cause premature transition, at least for Reynolds numbers between 16×10^6 and 20×10^6. The section drag coefficients of model 6 are extremely high as compared with those of the other models for which data are presented in figure 16. The extreme waviness of this model as shown in figure 17 (e) presents an example of waviness sufficiently severe to cause premature transition, at least for Reynolds numbers above 8×10^6. It may be noted in table I that model 6 was constructed with spanwise hat-section stiffeners, the flanges of which were rather heavy with respect to the airfoil skin The other models for which data are presented in figure 16 were constructed with chordwise stiffeners. Somewhat greater difficulty may be experienced in constructing airfoils with fair contours when spanwise stiffeners that are heavy with respect to the airfoil skin are used.

Photographs of model 12 (the NACA 23015 (approx.) airfoil section) and model 13 (the NACA 23016 airfoil section) are presented as figures 18 and 19, respectively. The variation of section drag coefficient with Reynolds number for these two models is presented in figure 20 and the waviness measurements are presented in figure 21.

The lower drag of the two models was obtained with model 12, which had a section drag coefficient of 0.0057 at a Reynolds number of 20×10^6 (fig. 20). A fair and smooth NACA 230-series airfoil would probably have approximately the same section drag coefficient as model 12, at least up to Reynolds numbers of approximately 20×10^6. The waviness existing on model 12 (fig. 21 (a)) in the region where laminar flow might ordinarily be expected—that is, up to approximately 0.12c on the upper surface and 0.20c on the lower surface—evidently had no adverse effects on the drag of this model up to Reynolds numbers of approximately 20×10^6. Because the waviness characteristics of models 12 and 13 were similar as far back from the leading edge as approximately 0.40c (figs. 21 (a) and 21 (b)), the waves existing on model 13 in the laminar-flow region also probably had little effect on the drag characteristics. The extreme waviness of model 13 behind the 0.40c position was probably due to the very thin skin of this model (table I). The skin was known to vibrate considerably during the drag tests. It is possible, therefore, that such vibration was responsible for the fact that model 13 had generally higher drags than model 12.

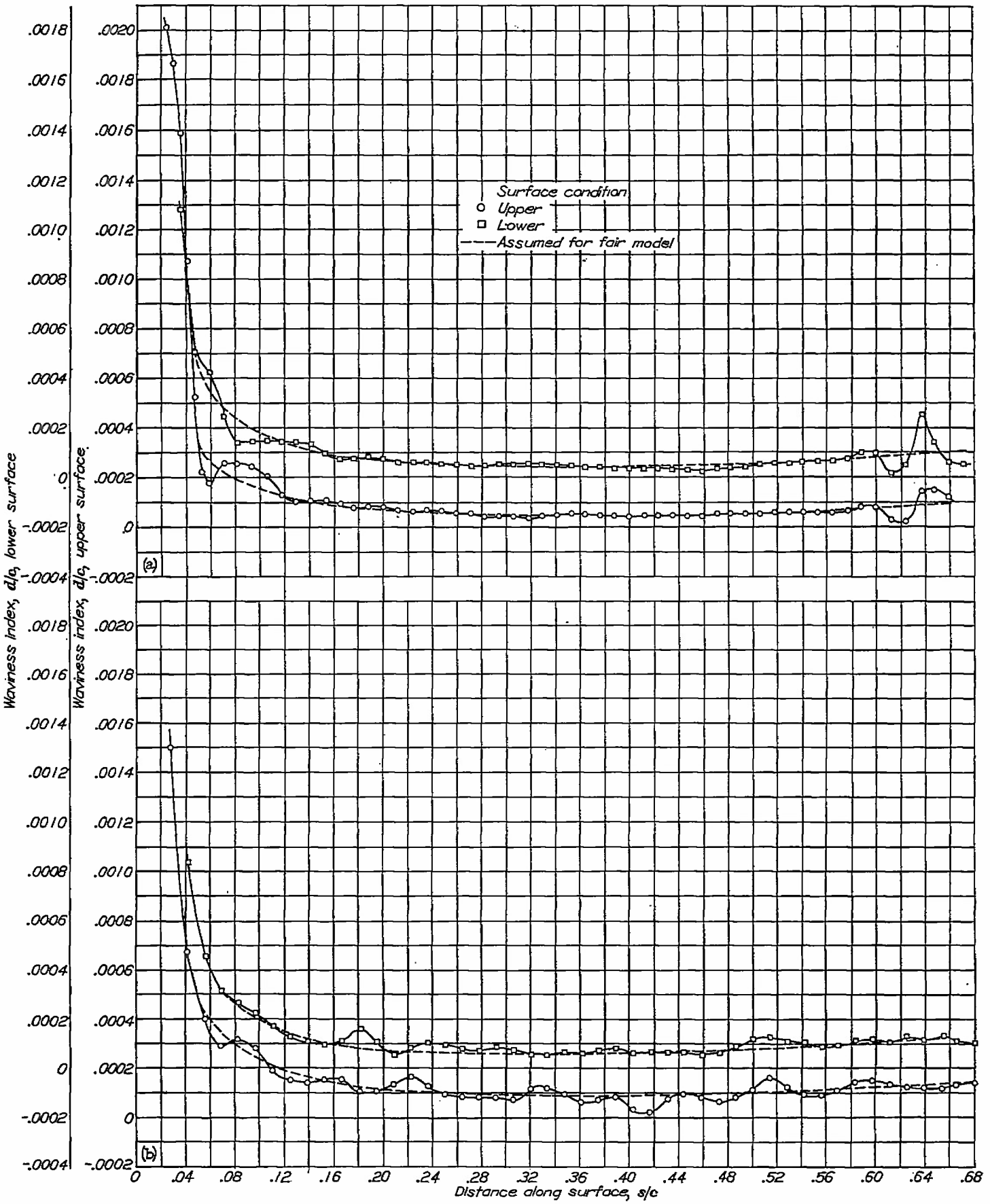

(a) Surface waviness of NACA 66(215)-116 $\left\{\begin{matrix}\alpha=1.0,\ c_{l_i}=0.2\\ \alpha=0.6,\ c_{l_i}=-0.1\end{matrix}\right\}$ practical-construction airfoil section. Model 5.

(b) Surface waviness of NACA 66(215)-(1.25)16 practical-construction airfoil section. Model 9.

FIGURE 17.—Waviness characteristics of some smooth NACA 6-series practical-construction airfoil sections.

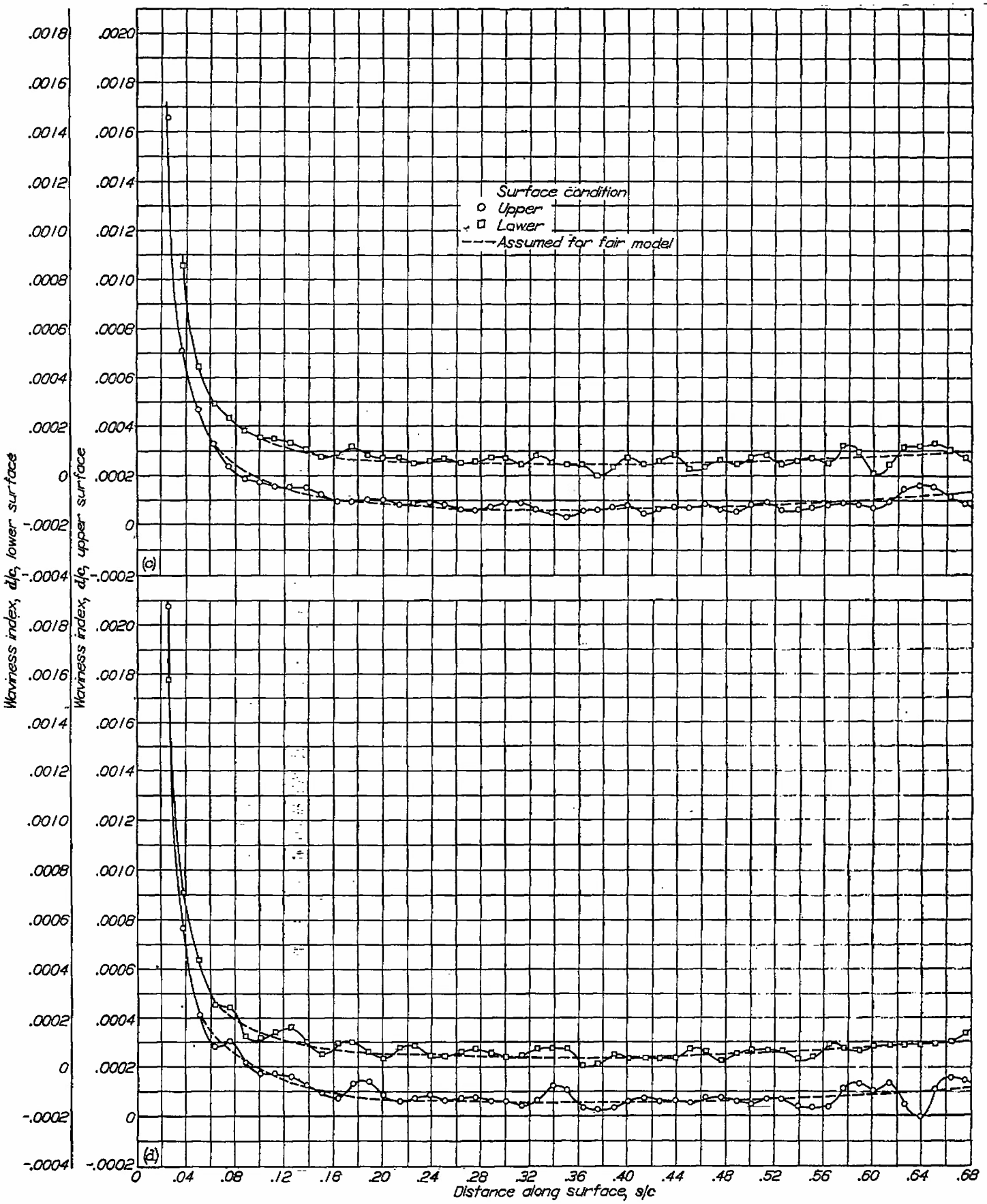

(c) Surface waviness of NACA 66,2-115 practical-construction airfoil section. Model 10.
(d) Surface waviness of NACA 66,2-115 practical-construction airfoil section. Model 11.

FIGURE 17.—Continued.

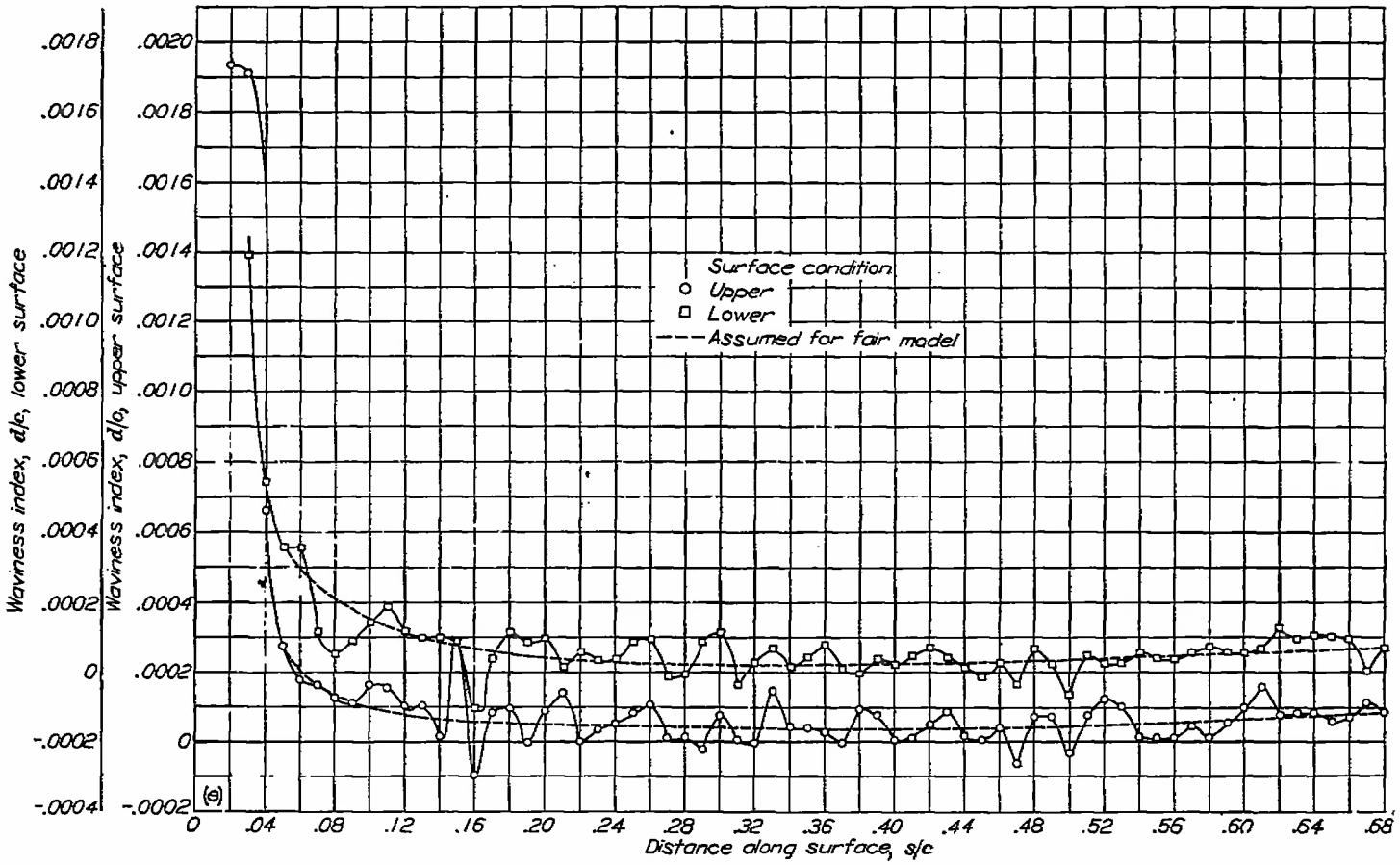

(e) Surface waviness of NACA 66(215)-116 practical-construction airfoil section Model 6.
FIGURE 17.—Concluded.

FIGURE 18.—Model of NACA 23015 (approx.) practical-construction airfoil section with camouflage-painted surfaces. Model 12.

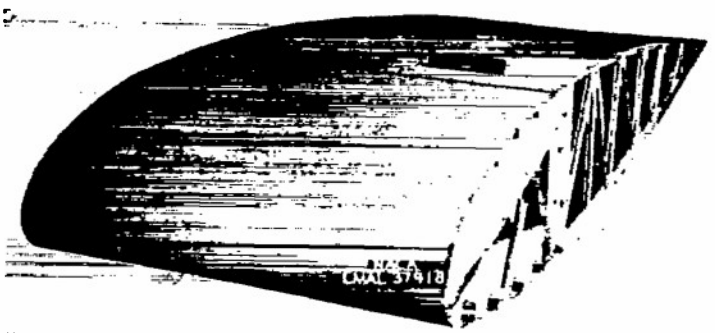

FIGURE 19.—Model of NACA 23016 practical-construction airfoil section with camouflage painted surfaces. Model 13.

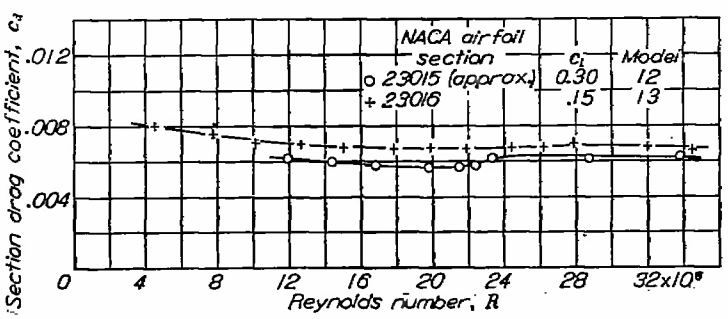

FIGURE 20.—Drag characteristics of some smooth 230-series practical-construction airfoil sections with some surface waviness.

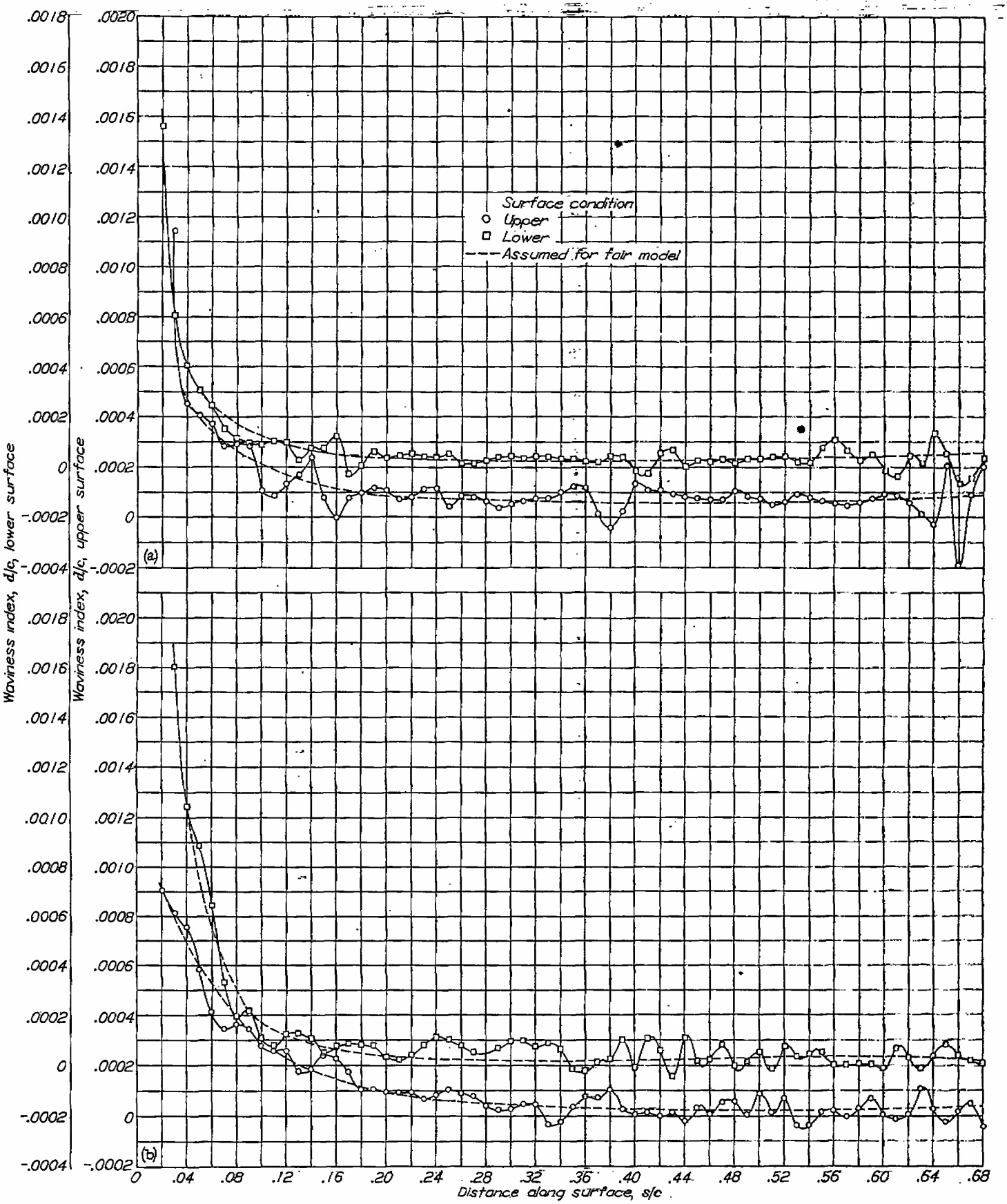

(a) Surface waviness of NACA 23015 (approx.) practical-construction airfoil section. Model 12.
(b) Surface waviness of NACA 23016 practical-construction airfoil section. Model 13.

FIGURE 21.—Waviness characteristics of some smooth NACA 230-series practical-construction airfoil sections.

An example of a model that shows the effect of deviation from true airfoil contour over a large part of the chord is model 4, for which drag data are presented in figure 22 and surface unfairness (deviation from true contour) and pressure-distribution measurements are presented in figure 23. The effect of deviation from contour (fig. 23 (a)) on the pressure distribution was to increase the velocities over the first 50 percent chord above the theoretical velocities and to move the minimum pressure point from 0.60c to approximately 0.50c (fig. 23 (b)). A comparison of the drag characteristics of model 4 with those of model 7 (fig. 22) shows that the deviations from contour had little effect on the drag of model 4 at Reynolds numbers below 26×10^6 but at Reynolds numbers greater than 26×10^6 the drag of model 4 tended to be greater than that of model 7.

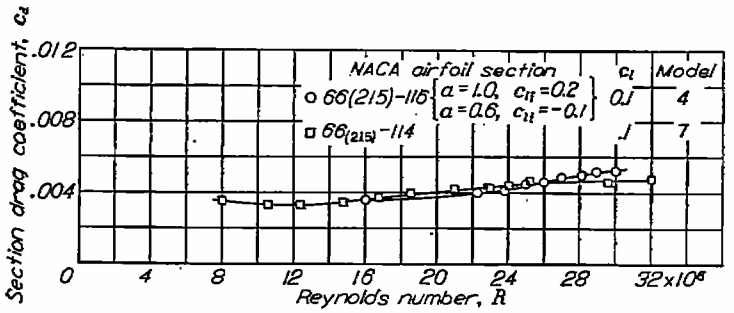

FIGURE 22.—Drag of NACA 66(215)-116 $\left\{\begin{matrix}a=1.0,\ c_{l_i}=0.2\\ a=0.6,\ c_{l_i}=-0.1\end{matrix}\right\}$ practical-construction airfoil section, surfaces painted and glazed, compared with drag of faired NACA 66(215)-114 practical-construction airfoil section.

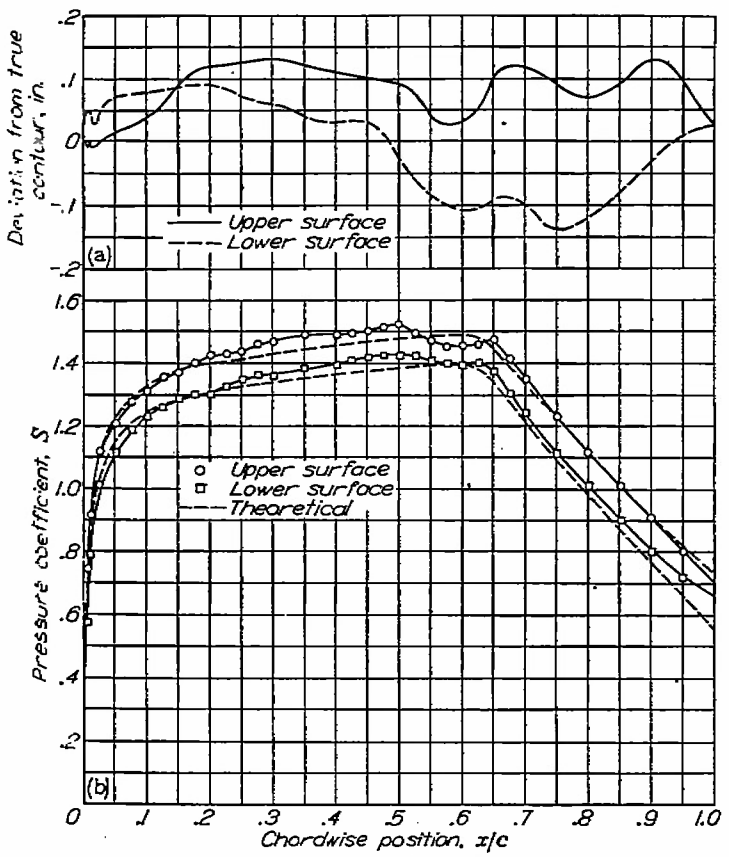

(a) Surface unfairness, painted and glazed condition.
(b) Pressure distribution, $c_l \approx 0.1$.

FIGURE 23.—Surface unfairness and pressure distribution for NACA 66(215)-116 $\left\{\begin{matrix}a=1.0,\ c_{l_i}=0.2\\ a=0.6,\ c_{l_i}=-0.1\end{matrix}\right\}$ practical-construction airfoil section. Model 4.

Comparison of NACA 6- and 230-series airfoil section.—In order to determine whether the relative merits of airfoil sections of different series are masked by construction defects, the drag characteristics of several NACA 6- and 230-series airfoil sections have been compared.

Drag data are presented in figure 24 for models 2, 8, 12, and 13. Figure 24 (a) shows little difference in the section drag coefficients of the NACA 66(215)-214 (approx.) and 23016 airfoil sections in the original conditions, although the drag of the NACA 66(215)-214 (approx.) airfoil section is much lower than that of the NACA 23016 airfoil section in the finished condition. Comparison of the drags of the NACA 66(2x15)-116 and 23015 (approx.) airfoil sections in figure 24 (b) shows appreciable difference in drag of the models in the original condition but a much greater difference in the smooth condition. From these data the differences in drag associated with smooth NACA 230- and 6-series airfoil sections, as constructed, appear to be considerably reduced if not entirely masked.

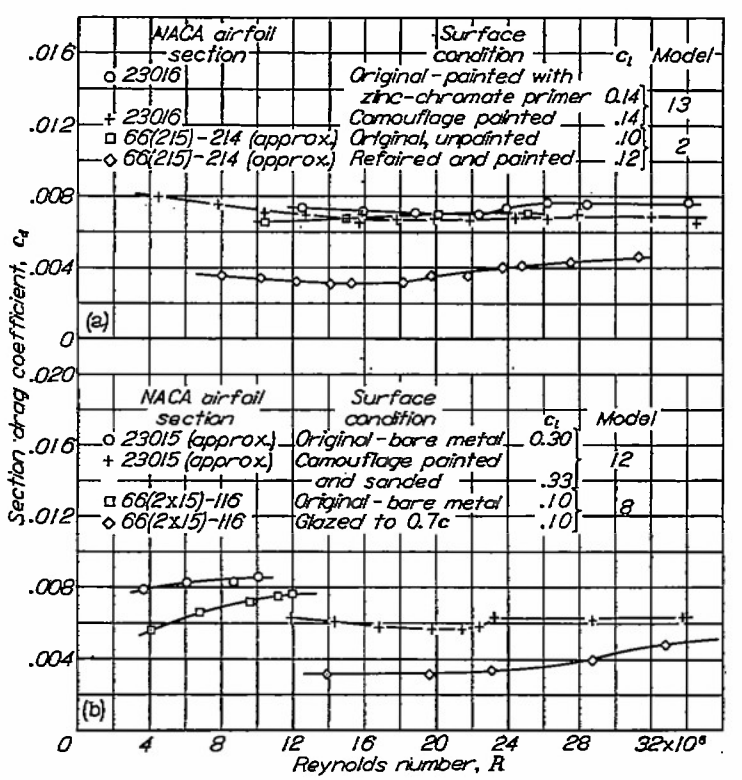

(a) NACA 23016 and 66(215)-214 (approx.) airfoil sections.
(b) NACA 23015 (approx.) and 66(2x15)-116 airfoil sections.

FIGURE 24.—Comparison of drag characteristics of some 230- and 6-series airfoils.

Comparison of drag of airplane wing and practical-construction wing model.—A comparison has been made in figure 25 of the drag characteristics of a smooth practical-construction wing model having the NACA 66(215)–214 (approx.) airfoil section and a smooth test panel of an airplane wing having the NACA 66(215)–2(14.7) airfoil section. The airplane wing panel had been carefully faired to eliminate any protuberances or waviness due to wing joints or access doors. Both the airfoils used had NACA 66-series sections with thickness ratios of approximately 0.14.

In figure 25 at section lift coefficients below 0.3, the practical-construction wing model had lower drag than the airplane wing panel; whereas, at higher section lift coefficients the reverse was true. Since data for the airplane wing were obtained in flight, it is difficult to determine whether the higher drags associated with the airplane wing were due to buckling under load at the time that the data were obtained. It is possible, however, that waviness on the airplane wing existed relatively far back on the wing surface, and the adverse effects of such waviness were noticeable only at the lower section lift coefficients. Furthermore, similar waviness that was not large enough to cause premature transition under the favorable pressure gradient existing at the low section lift coefficients might have existed closer to the leading edge of the NACA 66(215)–214 (approx.) airfoil section but, under a less favorable pressure gradient at section lift coefficients above 0.3, such waviness might well have resulted in premature transition.

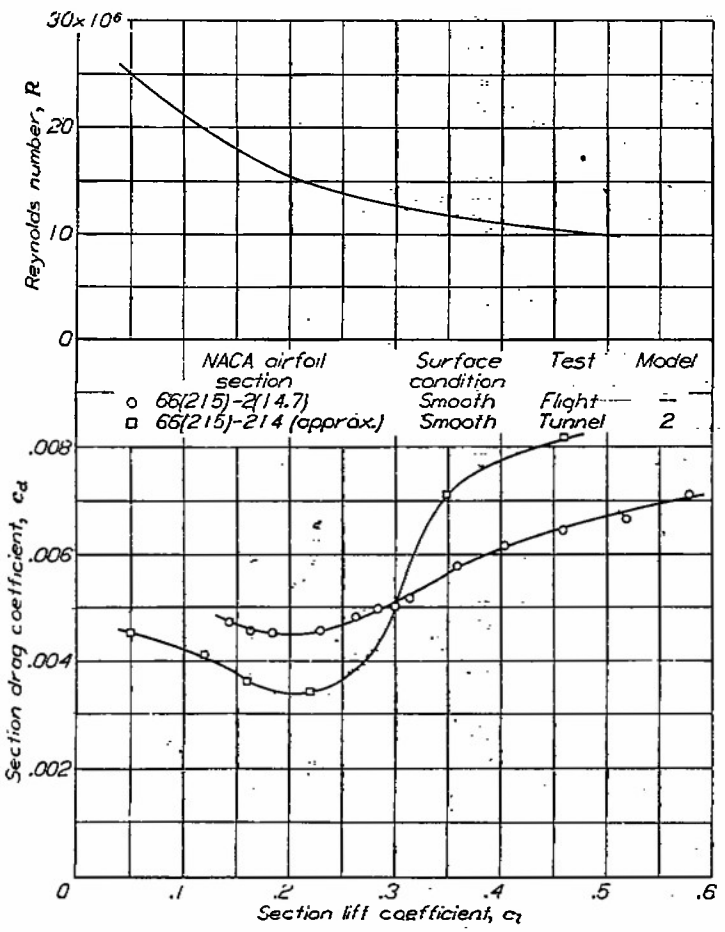

FIGURE 25.—Comparison of drag characteristics of smooth test panel of airplane wing with that of smooth practical-construction wing model.

EFFECTS OF COMPRESSIVE LOAD AND DE-ICERS

Effect of compressive load.—The effect of deformation, or waviness, of the wing skin in flight presents a further obstruction to the realization of the design drag characteristics of airfoil sections. For this reason two wing panels, models 9 and 14, constructed at the Langley Laboratory of the NACA (reference 5), were designed to retain their true contour under loads ordinarily encountered in flight. The drag characteristics of these sections were measured before being subjected to compressive load. Compressive load was then alternately applied and removed, each successive load exceeding the last, until some failure of the wing was detected. With both wings, local slippage of the rivet heads or crushing of the skin around the rivets comprised the sole permanent deformation of the models. The drag characteristics of the models were then determined again. For a third airfoil model, model 15, which was constructed by a manufacturer, the drag was measured while compressive load was being applied.

Photographs of model 14 (the NACA 66(215)–(1.25)16 airfoil section) and model 15 (the NACA 65(216)–215 (approx.) airfoil section) are presented as figures 26 and 27, respectively. The drag characteristics of models 9, 14, and 15 are presented in figure 28. With the exception of the stiffener spacing between spars, models 9 and 14 were identical (table I). These models were unpainted but were glazed locally at the front spar and over the rivet heads. Inspection of figures 28 (a) and 28 (b) shows that the drag coefficients for these two models at Reynolds numbers above 20×10^6 were somewhat lower for the after-loading condition than for the before-loading condition. When the model surfaces were cleaned and refinished, after being subjected to the compressive loads, the models were probably made smoother than for the aerodynamic tests conducted before the compressive loads were applied. The slight protuberances of the rivet heads caused by the compressive loads, however, were not removed by the finishing process. On the basis of these two tests, the type of construction employed appeared sufficiently good to allow realization of the section drag coefficients usually associated with NACA 66-series airfoil sections at Reynolds numbers up to approximately 30×10^6. In addition, model 9, with stiffeners spaced 3 inches on centers, appeared to offer no particular aerodynamic advantage over model 14, with stiffeners spaced 6 inches on centers; and the adverse effects of the compressive loads appeared to be so small that these effects were completely masked by slight improvements in surface finish.

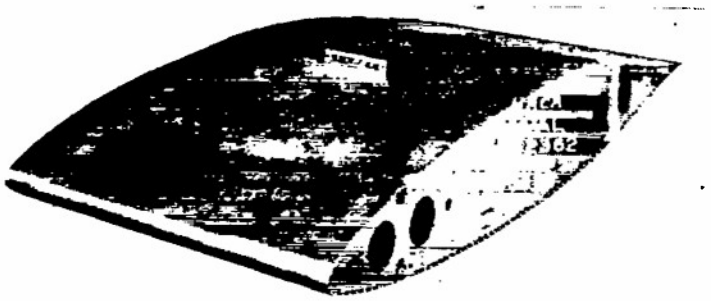

(a) Front top view.

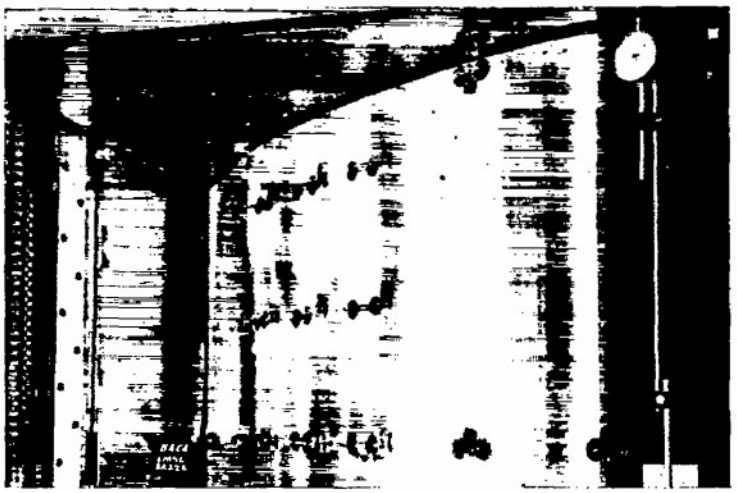

(b) View of model being subjected to compressive load in 1,200,000-pound testing machine.

FIGURE 26.—Model of NACA 66(215)-(1.25)16 practical-construction airfoil section. Model 14.

Model 15, designed for the wing of a fighter bomber, was subjected to compressive loads up to a load that was thought to correspond to a load of 1.5g for the airplane. These loads were applied by a hydraulic jack mounted within the wing, which was fixed in the tunnel. Figure 28 (c) shows that with the model under a load sufficient to produce slight waviness (1.0g) little or no effect on the drag was found, but that with the model under a load great enough to produce some permanent deformation of the skin (1.5g) waves existed that were serious enough to bring about a sharp increase in drag at a Reynolds number of 20×10^6.

For the cases just considered, slight permanent set in the skin or rivets of the wings caused by compressive loads had little or no effect on the drag characteristics. While the wing was experiencing load sufficient to produce such deformation, however, the drag characteristics were adversely affected to a considerable extent.

Effects of de-icers.—Data are presented in figure 29 for two airfoil models equipped with leading-edge de-icer boots. These boots consisted of rubber sheets attached to the wing surface and were tapered to a fine edge on the upper and lower surfaces of the airfoil at the point where they faired into the wing contour.

(a) Front top view.

(b) Rear top view.

FIGURE 27.—Model of NACA 65(216)-215 (approx.) practical-construction airfoil section. Model 15.

A 0.075c de-icer boot on the leading edge of model 15 (the NACA 65(216)-215 (approx.) airfoil section) caused a section-drag-coefficient increment amounting to 0.0025 or 0.0030 (fig. 29 (a)), whereas a similar 0.15c de-icer boot caused increments of approximately 0.0040. A 0.10c de-icer boot on model 12 (the NACA 23015 (approx.) airfoil section) caused section-drag-coefficient increments of approximately 0.0010 (fig. 29 (b)). The total section drag coefficients of the NACA 6-series with the 0.075c de-icer boot and the NACA 23015 airfoil with the 0.10c airfoil de-icer boot were approximately 0.0070 at Reynolds numbers between 10×10^6 and 32×10^6, whereas the drag of the NACA 6-series airfoil with the 0.15c de-icer boot was somewhat greater, at least at Reynolds numbers up to 10×10^6. It would appear, then, that not only are the drags of airfoil sections increased considerably by the addition of leading-edge de-icer boots but that the differences in drag usually associated with airfoil sections of different series are masked, at least for thickness ratios of approximately 15 percent.

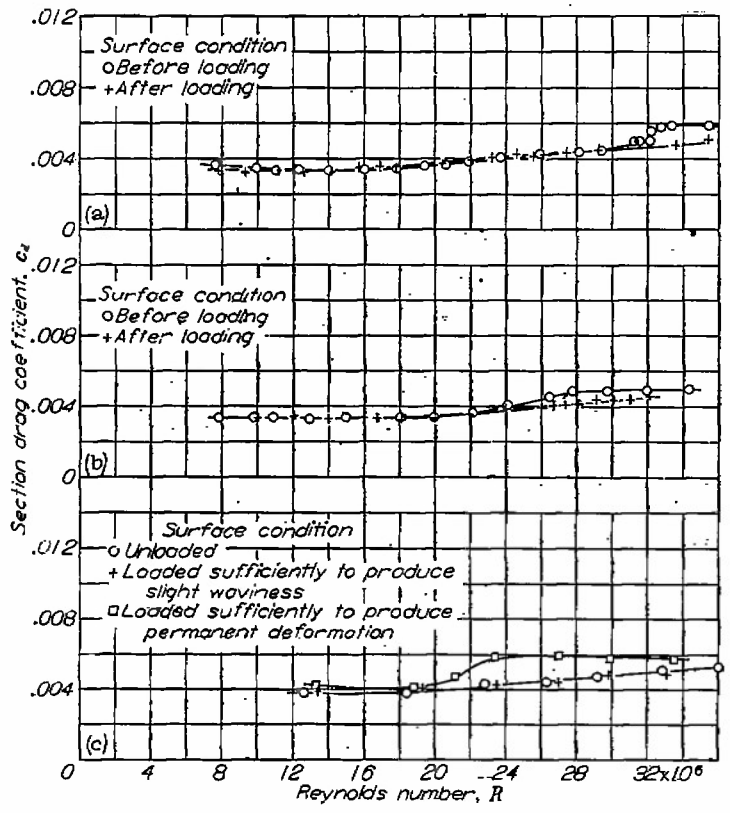

(a) NACA 66(215)-(1.25)16 airfoil section with chordwise hat-section stiffeners spaced 3 inches on centers. c_l=0.14. Model 9.
(b) NACA 66(215)-(1.25)16 airfoil section with chordwise hat-section stiffeners spaced 6 inches on centers. c_l=0.16. Model 14.
(c) NACA 65(216)-215 (approx.) airfoil section. c_l=0.3. Model 15.
FIGURE 28.—Effect of compressive load on drag characteristics of airfoils.

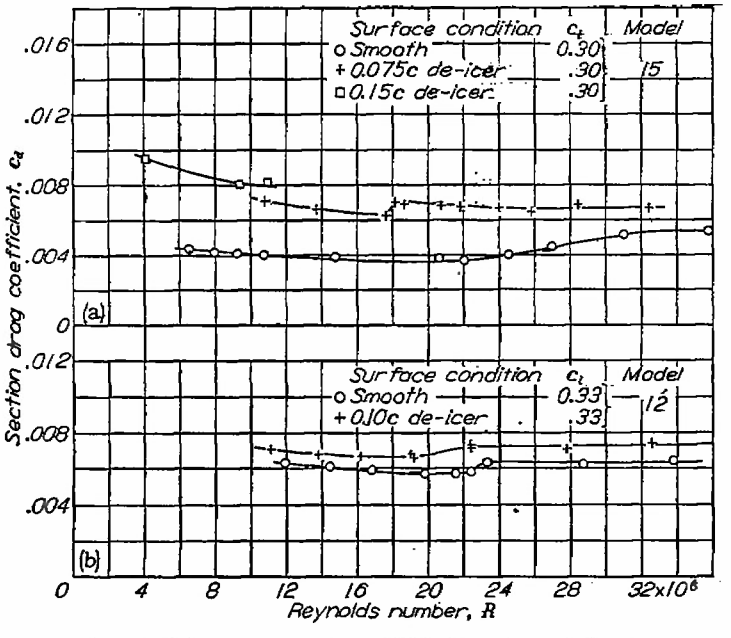

(a) 0.075c and 0.15c de-icer boots on NACA 65(216)-215 (approx.) airfoil section.
(b) 0.10c de-icer boot on NACA 23015 (approx.) airfoil section.
FIGURE 29.—Effect of de-icer boots on drag characteristics of airfoil sections.

CONCLUSIONS

From the analysis of the drag characteristics of practical-construction wings, quantitative data were obtained that indicated the size, number, and locations of surface waves sufficient to induce premature transition at Reynolds numbers greater than 9×10^6, at Reynolds numbers greater than 16×10^6, at Reynolds numbers greater than 24×10^6, and for waves that did not bring about premature transition, at least for Reynolds numbers up to approximately 50×10^6. In addition, the following conclusions were obtained:

1. When spar joints or similar surface discontinuities occurred in a region of normally laminar flow, the section drag coefficients of several practical-construction wings in the as-received condition ranged from 0.0062 to 0.0086. Improvement in surface smoothness and decrease of surface waviness at the spar joint often decreased the section drag coefficients by an amount ranging from 0.0022 to 0.0035, depending upon the magnitude of surface roughness and waviness in the as-received condition. In some cases nearly half the decrease in drag coefficient was associated with decreases in surface waviness.

2. Smooth practical-construction models with relatively heavy skin and with the spar joint placed at or behind the most rearward position at which laminar flow might be expected yielded drag coefficients that closely approached those of a fair and smooth airfoil section.

3. It was possible to calculate with reasonable accuracy the variation of section-drag coefficient with Reynolds number, at least between Reynolds numbers of 30×10^6 and 50×10^6, for two smooth NACA 6-series airfoil models on which the surface waviness had been reduced beyond the point where an effect was noticeable on drag. It was assumed for the calculations that transition occurred at a value of the Reynolds number based on the boundary-layer thickness R_δ between 8000 and 9000, if transition did not occur as a result of an unfavorable pressure gradient. Some existing flight measurements of boundary-layer transition at moderately high Reynolds numbers indicated that this range of values of R_δ was within that found in flight.

4. The improvement in surface smoothness and waviness brought about by glazing, painting, and minor refairing was in most cases sufficient to reduce the drags of unfinished practical-construction wings to values closely approaching those for a fair and smooth airfoil model of corresponding section, at least at Reynolds numbers up to approximately 20×10^6.

5. The differences in drag usually associated with airfoil sections of different series, if not entirely masked, were considerably reduced by construction irregularities.

6. Slight permanent set of the wing skin or rivets caused by compressive loads produced little or no adverse effect on the drag characteristics of two wing sections designed to retain true contours under loads usually encountered in

flight. While the wing was experiencing load sufficient to produce such deformation, however, the drag of the wing was considerably higher than the drag of the unloaded wing.

7. Airfoil sections having thickness ratios of approximately 15 percent and equipped with de-icer boots on the leading edge had section drag coefficients of approximately 0.0070 over a range of Reynolds number from 10×10^6 to 32×10^6. This value of the section drag coefficient, furthermore, seemed to be independent of the airfoil section upon which the boot was mounted.

LANGLEY MEMORIAL AERONAUTICAL LABORATORY,
NATIONAL ADVISORY COMMITTEE FOR AERONAUTICS,
LANGLEY FIELD, VA., *July 11, 1946*.

REFERENCES

1. Abbott, Ira H., Von Doenhoff, Albert E., and Stivers, Louis S., Jr.: Summary of Airfoil Data. NACA Rep. No. 824, 1945.
2. Braslow, Albert L.: Investigation of Effects of Various Camouflage Paints and Painting Procedures on the Drag Characteristics of an NACA $65_{(421)}$-420, a=1.0 Airfoil Section. NACA CB No. L4G17, 1944.
3. Tetervin, Neal: A Method for the Rapid Estimation of Turbulent Boundary-Layer Thicknesses for Calculating Profile Drag. NACA ACR No. L4G14, 1944.
4. Jacobs, E. N., and Von Doenhoff, A. E.: Formulas for Use in Boundary-Layer Calculations on Low-Drag Wings. NACA ACR. Aug. 1941.
5. Davidson, Milton, Houbolt, John C., Rafel, Norman, and Rossman, Carl A.: Preliminary Aerodynamic and Structural Tests Showing the Effect of Compressive Load on the Fairness of a Low-Drag Wing Specimen with Chordwise Hat-Section Stiffeners. NACA ACR No. 3L02, 1943.

TABLE I.—MODEL DATA AND DESCRIPTIONS

Model	NACA airfoil section	Manufacturer	Chord (in.)	Condition	Figure	Photograph	Model description
1	65(216)-3(16.5) (approx.)	A	100	Bare metal Original, camouflage painted Sanded Glazed to 0.12c Upper surface glazed behind 0.12c Lower surface glazed to 0.12c Upper surface painted to 0.71c Lower surface painted to 0.12c Both surfaces painted to 0.71c	 8 (a) 8 (a) 8 (a) 8 (a) 8 (a) 8 (a)	2	Spars at 0.12c, 0.45c, and 0.71c. Chordwise channel-section stringers and spanwise Z-section stringers on upper surface; chordwise channel-section stringers on lower surface. Channel-section stringers 0.088 inch thick on upper surface and 0.048 inch thick on lower surface. Z-section stringers 0.107 inch thick. Skin of 0.094-inch thickness fastened to spars with Phillips head screws. Countersunk rivets.
2	66(215)-214 (approx.)	B	81	Bare metal Glazed and painted Refaired	8 (b), 24 (a) 8 (b) 8 (b), 24 (a), 25	3	Spars at 0.35c and 0.70c. Metal skin fastened with flush-type rivets.
3	66(215)-116	C	84.9	Original, bare metal Glazed to 0.32c Painted to 0.32c Glazed and painted behind 0.32c Painted all over Painted and partly refaired	8 (c) 8 (c) 8 (c) 8 (c) 8 (c) 8 (c)	4	Single spar at 0.32c. All-metal skin.
4	66(215)-116 {a=1.0, c_H=0.2 / a=0.6, c_H=−0.1}	D	85	Original, painted with zinc-chromate primer. Painted Glazed	8 (d) 8 (d) 8 (d), 22, 23	 5 	Single spar just behind 0.60c. Skin of 0.125-inch thickness forward of spar stiffened on each surface with one chordwise flush-riveted stiffener. Riveted joint at leading edge.
5	66(215)-116 {a=1.0, c_H=0.2 / a=0.6, c_H=−0.1}	D	85	Original, painted with zinc-chromate primer. Painted and glazed	8 (e), 16, 17 (a) 8 (e)	6 	Same as model 4.
6	66(215)-116	C	100	Original, covered with fabric surfacer Sanded Bare metal Glazed to 0.15c Glazed to 0.45c	8 (f) 8 (f) 8 (f) 8 (f), 16, 17 (e) 8 (f)	 7	Spars at 0.15c and 0.45c. One J-section stiffener at 0.04c of 0.068-inch thickness. Spanwise hat-section stiffeners 0.047 inch thick spaced 0.05c on centers between spars. Skin 0.05 inch thick up to 0.45c. Ribs from rear spar to trailing edge.
7	$66_{(m)}$-114	C	85	As received, bare metal surfaces Both surfaces faired	10, 11 10, 11, 16, 22	9 	Spars at 0.081c, 0.373c, 0.688c. Behind front spar skin was 0.675 inch thick, built up of 0.5-inch balsa sandwiched between duralumin sheets. Skin cycle-welded to internal structure. Part of the airfoil ahead of the front spar formed of 0.125-inch duralumin sheet.
8	66(2x15)-116	E	99.2	Camouflage painted Original, bare metal Glazed to 0.7c Faired	13, 14, 16 24 (b) 24 (b) 13, 14	12 	Chordwise seam to 0.8c. Chordwise row of rivets from leading edge to trailing edge. Spar at 0.35c with forward part fastened by countersunk Phillips head screws.
9	66(215)-(1.25)16	F	72	Glazed	16, 17 (b), 28 (a)		Spars at 0.15c and 0.72c. Solid end ribs, false nose and tail ribs spaced at 6-inch intervals. Chordwise hat-section stiffeners spaced at 3-inch intervals between spars.
10	66, 2-115	G	80	Camouflage painted	16, 17 (c)		Spars at 0.125c and 0.585c. Skin 0.067 inch thick. Chordwise stiffeners between spars with false nose and tail ribs. Spot-welded construction.
11	66, 2-115	G	80	Camouflage painted	16, 17 (d)	15	Same as model 10 except flush-riveted construction.
12	23015 (approx.)	H	100	Camouflage painted Original, bare metal 0.10c de-icer	20, 21 (a), 24 (b), 29 (b). 24 (b) 29 (b)	18 	Spars at 0.105c and 0.605c. Skin 0.066 inch thick. Spanwise angle-section stiffeners ahead of front spar 0.056 inch thick. Metal skin fastened to interior structure by countersunk flush rivets.
13	23016	C	100	Camouflage painted Original, painted with zinc-chromate primer.	20, 21 (b), 24 (a) 24 (a)	19 	Single spar at 0.3c. Skin of 0.047-inch thickness forward of spar and 0.015-inch-thick skin behind spar. Spanwise J-section stiffeners ahead of spar 0.052 inch thick. Flush-riveted.
14	66(215)-(1.25)16	F	72	Glazed	28 (b)	26	Same as model 9 except chordwise stiffeners spaced 6 inches on centers.
15	66(216)-215 (approx.)	J	97.3	Glazed 0.075c de-icer 0.15c de-icer	28 (c), 29 (a) 29 (a) 29 (a)	27 	Spars at 0.215c and 0.615c. Skin approximately 0.0625 inch thick. Chordwise hat-section stiffeners spaced approximately 6 inches on centers between spars.

ATI-71 194

Langley Aeronautical Lab., Langley Air Force Base, Va. (910)
SUMMARY OF DRAG CHARACTERISTICS OF PRACTICAL CONSTRUCTION WING SECTIONS, by John H. Quinn Jr. 1948. 19 pp. UNCLASSIFIED

(Not abstracted)

DIVISION: Aerodynamics (2)
SECTION: Wings and Airfoils (6)
PUBLISHED BY: National Advisory Committee for Aeronautics, Washington, D. C.
DISTRIBUTION: U. S. Military Organizations request copies from ASTIA-DSC. Others route requests to ASTIA-DSC thru AMC, Wright-Patterson Air Force Base, Dayton, O. Attn: NACA.

L Quinn, John H. Jr.

ARMED SERVICES TECHNICAL INFORMATION AGENCY
DOCUMENT SERVICE CENTER